Assessing the mechanical properties of a cemented sand focusing on experimental and theoretical studies

Marina Bellaver Corte[1], *Lucas* Festugato[2], *Nilo Cesar* Consoli[2], *Erdin* Ibraim[3], and *Andrea* Diambra[3]

[1]*Catholic University of Rio de Janeiro, Department of Civil and Environmental Engineering, Rio de Janeiro, Brazil*
[2] *Federal University of Rio Grande do Sul, Department of Civil Engineering, Porto Alegre*
[3]*University of Bristol, Faculty of Engineering, Bristol, United Kingdom*
[#]*Corresponding author: marina@puc-rio.br*

ABSTRACT

The incorporation of cement to improve soil properties and attract the re-use of locally available materials has become a part of current geotechnical engineering projects. Its applicability varies from construction of pavement base layers, slope protection for earth dams, to support layer for shallow foundations. Unconfined behaviour might be used to evaluate the basic mechanical properties and efficiency of the cemented soils. The proposed relationship between porosity (η) and volumetric cement content (C_{iv}), presented as porosity cement index (η/C_{iv}), was shown to play an important role in the initial shear stiffness (G_0), tensile (q_t) and compressive (q_u) strength of cemented materials. This research aims to assess these parameters through experimental investigation and modelling predictions. Bender elements testing were carried out to assess the maximum initial shear stiffness (G_0) prior to specimens testing, and assessing G_0 evolution during cement hydration, focusing on the anisotropic/isotropic behaviour established during specimen moulding. Results show a good correlation between experimental and numerical data. It was also observed that cementation isotropises G_0 during curing.

Keywords: Cemented sand; porosity/cement index; strength; stiffness.

1. Introduction

When soil properties are inadequate for the task at hand, stabilization may be considered (Ingles and Metcalf 1972). The technique of stabilization adopted varies according to the soil and the properties required for engineering purposes, compaction of soils is known to be the first technique of soil stabilization ever used. More recent, the use of cement to soil stabilization showed to be a viable and sustainable approach to reach local soils with the requirements characteristics to engineering projects (Michell 1981; Consoli et al 2007 2008 2009a 2009b 2010 2016 2017 2019)

The improvement technique of mechanical properties for granular soils has presented an interesting use for this new material as pavement bases and support layers for shallow foundations (Consoli et al. 2009b). The use of compressive and tensile strengths of cemented materials is an easy way to verify the effectiveness of cementation. For unconfined compression tests, the specimen is subjected to direct loading, whereas in splitting tensile tests, also called Brazilian tests, the tensile strength is obtained indirectly from splitting tensile strength tests (Carneiro and Barcellos 1953). Even though the tensile strength is an indirect measure, the Brazilian test is widely used for cemented materials.

The compressive and tensile strength of artificially cemented sands obtained by unconfined compression and split tensile tests could estimate with the use of the porosity/cement index η/C_{iv} (Consoli et al 2007 2010). The η/C_{iv} index relates the porosity (η) of a compacted sample and the volumetric cement content (C_{iv}) to both unconfined compressive and splitting tensile strength. It is the first rational dosage methodology for soil– cement mixtures. Recently, Diambra et al. 2017, 2018 proposed theoretical derivations to explain the relationships the porosity/cement index has with unconfined compressive strength and splitting tensile strength, respectively.

The initial small strain stiffness of cemented soils is a useful design data for field applications, specially involving low stress levels as well as the material's quality control assessment. Consoli et al. 2010, 2017 shown that η/C_{iv} is an appropriate parameter to assess not only unconfined compressive strength (q_u) and splitting tensile strength (q_t) but also the maximum shear modulus (G_0). Later, Diambra et al. 2019 presented a theoretical justification for the existence of this relationship, which earlier was only through experimental data fitting only.

The anisotropy imposed by preparing the specimens by the method of undercompaction have been described by Ladd 1978. The vertical direction represents the direction of the tamping during sample preparation. This anisotropy induced on the specimens means that the change of the stress state leads to the change of the mechanical properties and parameters of the cemented sand when a complex load is applied in different directions (Arthur et al. 1977).

It is still limited the evaluation of the effect of vertically compacting specimen and its stiffness evolution during cement hydration. This research is proving the occurrence of straight relations among G_0, q_t, q_u, and adjusted η/C_{iv} for compacted sand - Portland cement blends, considering distinct moulding void ratio and cement contents. Further, verification of the observed results addressed with modelling predictions

from literature were observed. This research aims at addressing these issues.

2. Experimental Program

2.1. Materials

Hostun sand RF (S28) was used in this research, a standard European material for laboratory testing. This sand has a high amount of siliceous (SiO_2 > 98%) and it has angular to sob-angular grain shape. The grain size distribution is uniformly graded medium, its physical characteristics are mean grain size, D_{50} = 0.32mm, coefficient of uniformity, $C_u = D_{60}/D_{10} = 1.70$, coefficient of gradation, $C_g = (D_{30})^2/(D_{10}xD_{60}) = 1.1$, maximum and minimum void ratio, $e_{max} = 1.00$, $e_{min} = 0.62$, and specific gravity, $G_s = 2.65$.

The cementation agent used was a Portland cement of high initial strength (Type III, according to ASTM (2009)) and 7 days curing time was adopted in this research. Distilled water was used throughout the experimental investigation.

2.2. Moulding and curing of specimens

For the unconfined compressive and tensile strength tests, cylindrical specimens with 5 cm diameter and 10 cm height were prepared. With the mixture, material was divided into three portions (one for each layer of the specimen). Two small portions of the mixture were taken for moisture content determination. The specimen was then statically compacted in three layers inside a cylindrical acrylic mould, with a target mark to achieve the target dry density. The top of each layer was scarified to improve bonding between layers. The bottom and the last layer were prepared including the formation of a blank space exactly like the bender element that would be later inserted in the sample for testing. After compaction, the sample was immediately removed from the mould with an extractor. The sample was then weighted and sealed with plastic film. Samples were cured for six days in the laboratory, where the temperature and humidity were controlled (22°C ± 2°C and 60%). On the sixth day, the sample was measured before immersion in water for 24 hours, minimizing suction effect (CONSOLI et al. 2007 2010 2012a 2012b). Before testing for compressive or tensile strength, specimens were weighted again, and wave propagation tests were conducted with Bender Elements.

Differing from the cylindrical specimens, cubical ones were manufactured to be bench tested with bender elements. After compaction, specimen was carefully removed from mould and set up on a 3D printed cage, specifically design to keep the bender elements in place. Insertion of bender were made with a thin needle and 3 pairs were inserted, one in each direction. Cage, specimen and benders were sealed and were not removed from bag.

To be considered for testing, the samples had to comply with the following: dry density within ±1% of target value; moisture content within ±0.5% of the target value; diameter within ±0.5 mm; height within ±1 mm.

2.3. Splitting tensile and unconfined compression test

Splitting tensile and unconfined compression tests followed standard ASTM C496 (ASTM 2011b) and ASTM C39 (ASTM 2010), respectively. Tests were performed using a triaxial apparatus without the confinement system (Fig 1). Load cell had a maximum load of 5 kN and the imposed displacement rate was 1.0 millimetre per minute according to the ASTM D 1633.

The adopted testing strategy to investigate the behaviour of cemented sand under multiple loading conditions started with the determination of the η/C_{iv} index. Distinct cement contents and porosities were adopted to complete a wide range of this curve for unconfined compressive and tensile strength. Table 1 presents the set of specimens prepared for this part of the research. For each porosity and cement content, two samples were prepared. In total, 22 samples were performed for the unconfined compression test and 22 for the split tensile test.

Table 1. Sample dosages prepared for the unconfined tests

e	C (%)	ω (%)	Curing time (days)	Number of specimens
0.89	1.7, 3.4, 7			12
0.816	1.7, 3.4, 7			12
0.748	1.7, 3.4, 7	10	7	12
0.90	2.3			4
0.71	1.8			4

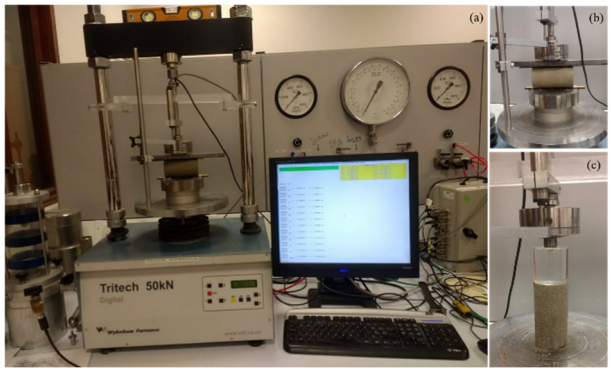

Figure 1. Triaxial frame used for the (a) and (b) split tensile strength; (c) unconfined compression strength.

2.4. Stiffness Measurements with bender elements testing

In previous testing, all samples prepared for the unconfined tests (compression and tensile) had their shear wave velocity measured through bender elements testing. Also, in order to obtain the stiffness evolution with the hydration of the cement, cubical samples were prepared, and three pairs of bender elements were inserted in the six faces of the cube sample (Fig 2). This procedure was adopted to specimen with same η/C_{iv}

target of 47.2 (e=0.90 and C=2.3%; e=0.71 and C=1.8%). In the first week of the sample curing, measurements were made every day. As the time of curing passed, the measurements were carried out every two days until no variation of the wave response was detected.

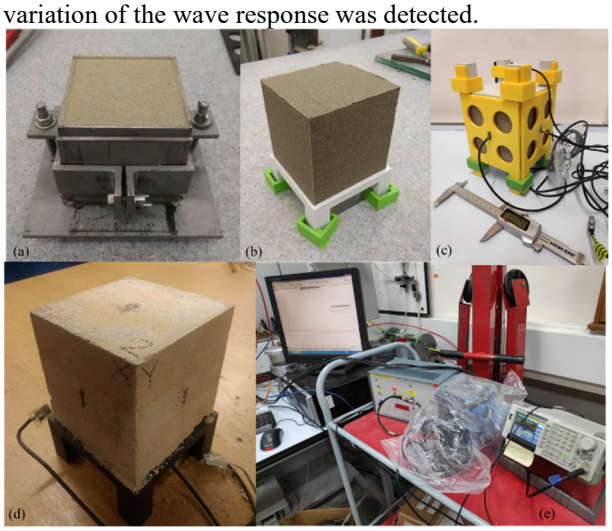

Figure 2. (a) Sample inside the mould; (b) sample positioned in the cage; (c) sample with the bender elements inserted; (d) sample after testing; (e) sample connected to oscilloscope and PicoScope.

3. Experimental Results and Analysis

3.1. Effect of porosity/cement index on split tensile strength, unconfined compressive strength and initial shear modulus

For all specimen studied split tensile strength (q_t), unconfined compression strength (q_u) and initial shear modulus (G_0) increased as cement content (C) increased. Also, by reducing porosity (η) it was noticed an increase of the three analysed behaviour: split tensile and unconfined compression strength and initial shear modulus.

By using the cement content and porosity curves, it was not possible to adjust a single curve representing the observed results. The voids/cement ratio, defined by the porosity of the compacted mixture divided by the volumetric cement content was used to predict the behaviour of the cemented material (Consoli et al. 2007). An exponent function was adjusted to the curves (Fig 3 a, b c).

Fig. 3a presents the relationship between η/C_{iv} and the unconfined compressive strength (q_u) of the cemented Hostun sand with a good correlation (R2 = 0.91). Equation 1 presents the correlation obtained from the relationship:

$$q_u(kPa) = 4.3x10^4 \left(\frac{\eta}{C_{iv}}\right)^{-1.40} \quad (1)$$

As for the results obtained for the tensile strength (Fig. 3b), a correlation of $R^2 = 0.85$ was obtained and the equation from the adjustment is presented in Equation 2:

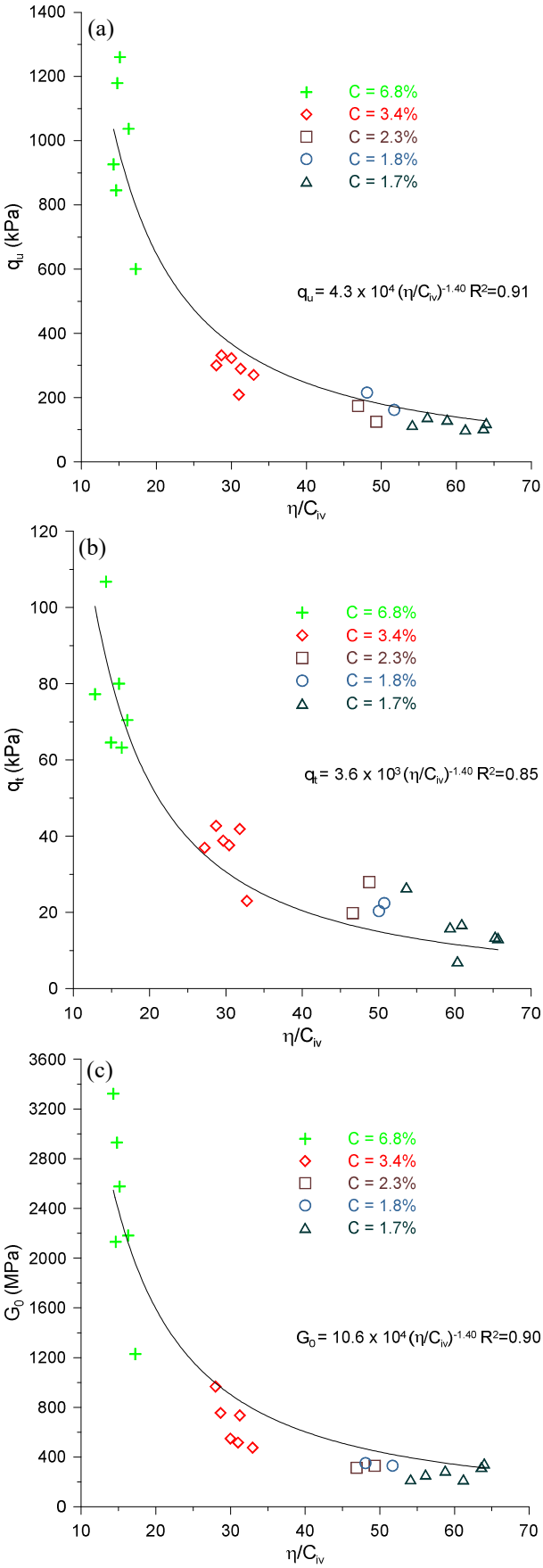

Figure 3. (a) Variation of unconfined compressive strength (q_u) with porosity/cement index (η/C_{iv}); (b) Variation of splitting tensile strength (q_t) with voids/cement ratio (η/C_{iv}); (c) Variation of the initial shear modulus (G_0) with adjusted porosity/cement index.

$$q_t(kPa) = 3.6x10^3 \left(\frac{\eta}{C_{iv}}\right)^{-1.40} \quad (2)$$

It is observed that Fig. 3a and 3b present similar trends. In order to check the relationship between q_t/q_u Equation 2 is divided for Equation 1 and presented in Equation 3:

$$\frac{q_t}{q_u} = \frac{3.6x10^3\left(\frac{\eta}{C_{iv}}\right)^{-1.40}}{4.3x10^4\left(\frac{\eta}{C_{iv}}\right)^{-1.40}} = 0.08 \quad (3)$$

It can be seen in Equation 3 that q_t/q_u is a scalar for the sand-cement blend, being independent of porosity, cement content, or porosity/cement index. There is a straight proportionality between tensile and compressive strengths, which is valid for the whole range of voids ratio and cement content studied in the present research program.

Therefore, it is possible to conclude that any rational dosage methodology considering the effect of different variables can be centered on tensile or compression tests, once they are intimately related through a scalar (0.08) for the sand-cement studied in the research.

The initial stiffness for the artificially cemented Hostun sand analysed by the porosity/cement index was presented in Fig. 3c. The correlation obtained was R^2 = 0.90 and the equation is presented in Equation 4.

$$G_0(MPa) = 10.6x10^4 \left(\frac{\eta}{C_{iv}}\right)^{-1.40} \quad (4)$$

It is observed that the adjusted porosity/cement index on the unconfined compressive strength on (q_u) and on the initial shear modulus (G_0) of the artificially cemented sand is quite similar, presenting comparable shapes of curves. As previous presented by Consoli et al. 2012, the relation of the G_0/q_u is presented in Equation 5. Variation of G_0/q_u is expressed by a constant, 2465.

$$\frac{G_0}{q_u} \cong 2465 \quad (5)$$

3.2. Modelling prediction

In this section the results obtained on the unconfined compressive strength and initial shear modulus are compared with theoretical derivations from literature.

3.2.1. Unconfined compressive strength: comparison with modelling

Based on the concept of superposition of failure strength contributions of the soil and cement phases, Diambra et al. 2017 provided a theoretical derivation for the unconfined compression strength of artificially cemented granular soils. The material granular matrix follows concepts of the critical state soil mechanics, and the strength of the cemented phase is described by the Drucker-Prager failure criterion. Through a volumetric averaging approach (Diambra et al. 2011 2013; Diambra and Ibraim 2015), the stress state of the cemented composite is derived from the stresses of its constituents at failure. To account for the soil matrix strength, the model requires the calibration of the parameter a, among others, which can be estimated through triaxial tests results. The parameter *a* links the peak strength of the soil matrix (represented using the density-dependent deviatoric stress and mean stress ratio q_m/p_m) to a state parameter [defined as the ratio between the porosity at the critical state (η_{cs}) and the current porosity (η)], as shown in Equation 6, where *M* represents the critical state strength.

$$\frac{q_m}{p_m} = M\left(\frac{\eta_{cs}}{\eta}\right)^a \quad (6)$$

The model developments yield in Equation 7 to describe unconfined compressive strength of cemented granular soils, where B_{iv} is the volumetric content of binder.

$$q_u = K\left[\frac{\eta}{(B_{iv})^{1/a}}\right]^{-a} \quad (7)$$

Diambra et al. 2017 also pointed out the similarity between Equations 5.6 and 5.7 and suggested that the exponents *D* and *E* in Equation 5.6 are dependent on the soil matrix related parameter *a*, $D=1/a$ and $E=-a$. The multiplying parameter *a* in Equation 6 is suggested to be the result of combined properties of the sand matrix and cement phase. According to the authors, the key governing parameters seem to be the frictional strength of the matrix and the strength of the cemented phase. The factor a is also affected by the exponent a, which is controlled by the soil matrix properties. The model used the critical state parameters for the soil matrix, these parameters were obtained from the data of Escribano 2014. The final model prediction of the authors is expressed in Equation 8.

$$q_u = \frac{6\mu_c\sigma_c{}^c}{k_c(1-\beta)+3(\beta+1)}\left[\frac{k_c - M\left(\frac{\eta_{cs}}{n}\right)^a}{3 - M\left(\frac{\eta_{cs}}{n}\right)^a}\right] \quad (8)$$

Table 2 presents the parameters used for the model. For the studied cemented soil matrixes, the observed value of a is 1.40, leading to *1/a* of 0.71, ~1.0, used in the experimental results.

Table 2. Sample dosages prepared for the unconfined tests

Symbol	Variable	Value
M	Critical state soil strength ratio	1.33 (ϕ'=33°)
η_{cs}	Critical; state soil porosity	0.48
A	Parameter governing dependence of soil	1.55
σ^c_c	Cement phase compressive strength	50 MPa
β	Uniaxial and extension cement strength ratio	-6
k_c	Cement stress ratio	4

Using the parameters presented in Table 2 and the Equation 8, the prediction parameter results in Equation 9. Fig. 4 presents the comparison of the experimental data and the modelling results, showing that modelling and data results in same order of magnitude and trend.

$$q_u = \frac{6\,{}^{C_{iv}}/_{100}\,50000}{4(1-(-6))+3((-6)+1)}\left[\frac{4-1.33\left(\frac{0.48}{\eta/100}\right)^{1.55}}{3-1.33\left(\frac{0.48}{\eta/100}\right)^{1.55}}\right] \quad (9)$$

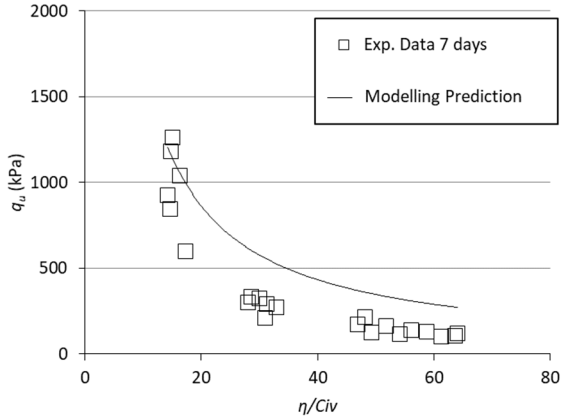

Figure 4. Comparison of q_u from results and model.

3.2.2. Initial shear modulus: comparison with modelling

Diambra et al. 2020 provided a theoretical justification for the existence of empirical power relationships governed by a porosity over cement content ratio for the evaluation of small strain stiffness. According to the authors, such a power relationship is a simplification of the well-established Hardin's type relationship for the initial small strain shear stiffness of cemented soils under unconfined loading conditions. Hardin's type relationships usually present materials stiffness as a function of void ratio (or porosity), structure related characteristic and mean effective stress. The power of the porosity η term in the empirical relationship accounts for the shape of the normal compression line (NCL) of the uncemented soil in the η-p' plane, while the cement content C_{iv} term accounts for the shift of the NCL of the cemented soil with respect to its uncemented NCL state. Diambra et al. 2020 showed the exponential term depending on the η may be seen as an approximation of the current Horslev pressure for uncemented soil and it is a term which accounts for the overconsolidation state or *f(e)* function of the material. The exponential term linked to the C_{iv} may represent the shift of the NCL for cemented soil and is a measure of the current state of cementation.

The theoretical model cited assumes that the composite cemented material is isotropic; the behaviour of the cemented soil at the failure is determined by superposing the strength contributions of the two phases: failure of the composite cemented soil occurs as a result of a simultaneous failure of both the cemented and soil matrix phases, and strain compatibility between the composite and its two phases applies.

The theoretical model requires the knowledge of the normal compression line for uncemented and cemented states. The NCL was obtained from previous studies in Hostun sand (Diambra, not published). Hostun sand and Osorio sand presented similar behaviour when NCL line were compared. For this reason and in order to use the theoretical proposition on the paper, it was assumed that the behaviour of 1.4% C_{iv} cemented Hostun sand was similar to 1.4% C_{iv} cemented Osorio sand obtained in the literature. For other cement contents the parameters were interpolated.

The model presents the following correlation expressed in Equation 10:

$$\frac{G_0}{p_r} = AD^m L^q \left(\frac{\eta}{C_{iv}{}^{q/(fm)}}\right)^{-fm} \quad (10)$$

From the analysis of the modelling prediction, the following values were obtained: AD^mL^q = 5xE^8, fm = 3.744, and q/fm = 0.5. The curve obtained from the model and the experimental results are combined in Fig. 5.

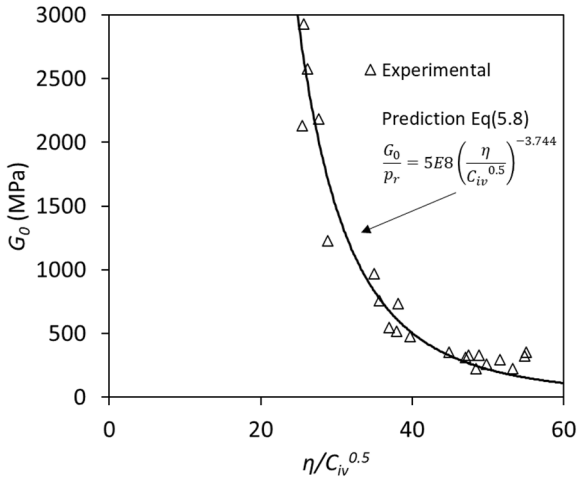

Figure 5. Comparison of G_0 from results and model.

3.3. Stiffness evolution

The cubical samples were prepared in order to analyse the evolution of the cemented specimen stiffness with the cement hydration. The specimens prepared for this purpose were left with the bender elements inserted in the specimen in order to avoid any kind of breakage during testing and moving the specimen. The samples were also placed in a tray with wheels to move the specimen and the reading system if needed. The measurements were made until no variation of the time of arrival of the wave was noticed.

Two samples are presented in this study. *z* direction corresponds to the vertical direction of the specimen (direction of specimen compaction) while *x* and *y* are the horizontal directions of the specimens. Only shear waves were recorded during the measurements. In the horizontal directions, represented in the research as *x* and *y*, the shear wave propagation was horizontally with horizontal propagation. This means that if an observer looks to the specimen; both faces the bender elements are vertical. As for the vertical direction, the representation is in *z* direction.

Fig. 6 shows the stiffness evolution of two specimens prepared with the same target η/C_{iv} (47.2) with two different proportions of the phases First specimen was prepared with 2.3% cement and void ratio of 0.90 (named C2.3e0.90 on this study). Second specimen preparation had 1.8% cement and void ratio of 0.71 (named C1.8e0.71). Specimen C2.3e0.90 on Fig 6a shows that the evolution of stiffness continues until day 16, at which point it remains constant. On specimen C1.8e0.71, the evolution of the stiffness reaches a constant value at day 3 (Fig 6c). When comparing the ratio between the

stiffness of *x* and *z* directions, it is observed that both reach a similar value within less than 3 days. From Fig. 6b and 6d, it is observed that the ratio between the stiffness the horizontal and vertical direction is close to unit (1) at the early days of measurements.

It was noticed that after compaction, the response is anisotropic and with the development of the cement hydration, the difference in the stiffness caused by the compaction of the specimens reduced over time. The evolution of the small stiffness for both specimens (Fig 6a and 6c) reveals that specimen C2.3e0.90 reaches a stabilized value after 16 days, while C1.8e0.71 gets to a constant level after only 3 days. These behaviour as addressed due to the cement content available in each specimen, reduced in specimen with 1.8% cement content. This time reduced was also linked to the fact that specimen with 0.71 void ratio presented a much easier handling and moving condition, due to its compaction; while, even with extreme care, removing from mould and inserting bender on specimen with high void ratio (e=0.90) presented some disturbance while handling. Although this stresses on specimen while handling, final measurements on both situations resulted in similar values: C2.3e0.90 was 555 MPa and C1.8e0.91 read 520 MPa.

4. Conclusions

The ratio between the amount of cement and porosity of cemented Hostun sand was observed to lead to unique curves expressing the unconfined compression strength, split tensile strength and initial shear moduli. The three curves were adjusted successfully to the same power (1.40). The ratio q_t/q_u obtained was 0.08. As for the ratio G_0/q_u, it was obtained 2465. Also, η/C_{iv} was used to define the specimen composition to the following analysis, focusing on the stiffness evolution with cement hydration over time of a lightly cemented sand with two specific void ratios and cement contents. An η/C_{iv} of 47.2 was targeted with (a) 2.3% cement and void ratio of 0.90 (C2.3e0.90) and (b) 1.8% cement and 0.71 void ratio (C1.8e0.71).

From the data presents in this paper, the following conclusions can be addressed:

- It was observed that the porosity/cement index curve provided a unique relationship with the unconfined compressive strength, tensile strength and initial stiffness of the artificially cemented Hostun sand. It was also observed that the three relationships had the same adjusted power on the η/C_{iv} (1.40).
- The prediction models used on the analysis presented compatible results when comparing to the experimental data.
- Regarding the evolution of the stiffness on the cemented samples, it was noticed that with the development of the cement hydration, the difference on stiffness caused by dumping compaction between vertical and horizontal specimen direction reduces over time. This was clear for the two cubical specimens analysed with small amounts of cement added. It was also observed that specimens with same η/C_{iv} resulted in similar final stiffness values.

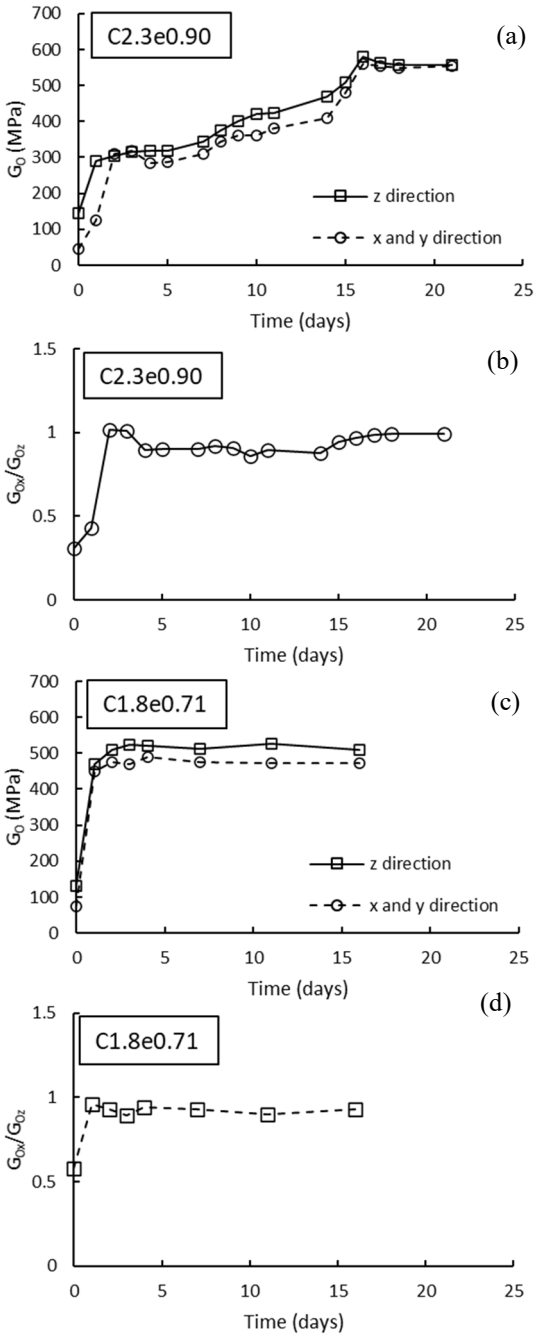

Figure 6. Stiffness evolution over time and comparison *z* and *x* and *y* directions: (a) and (b) e=0.90, C=2.3%; (c) and (d) e=0.71, C=1.8%.

Acknowledgements

The authors wish to express their gratitude to CNPq (research projects number 203293/2018-5), to FAPERGS-CNPq (PRONEX) and MEC/CAPES (PROEX) for their financial support of the research group. The authors also gratefully acknowledge the support provided by the UK Royal Academy of Engineering under the Newton Research Collaboration Programme (Grant NRCP1415/2/2).

References

American Society For Testing And Materials. ASTM D1633-17, Standard Test Methods for Compressive Strength of Molded Soil-Cement Cylinders, ASTM International, West Conshohocken, PA, 2017, www.astm.org

Arthur JRF.; Chua KS.; Dunstan, T. (1977) Induced anisotropy in a sand. Géotechnique, 27(1), 13–30

Carneiro FLB, Barcellos A (1953) Concrete tensile strength. Testing Research Laboratory Paris, France, Bulletin No. 13, pp 97–127

Consoli NC, Cruz RC, Floss MF, Festugato L (2010) Parameters controlling tensile and compressive strength of artificially cemented sand. J Geotech Geoenviron Eng 136(5):759–763

Consoli NC, Dallarosa F, Fonini A (2009b) Plate load tests on cemented soil layers overlaying weaker soil. J Geotech Geoenviron Eng 135(12):1846–1856

Consoli NC, Ferreira PMV, Tang CS, Marques SFV, Festugato L, Corte MB (2016b) A unique relationship determining strength of silty/clayey soils – Portland cement mixes. Soils and Foundations 56(6): 1082-1088

Consoli NC, Foppa D, Festugato L, Heineck KS (2007) Key parameters for strength control of artificially cemented soils. J Geotech Geoenviron Eng 133(2):197–205

Consoli NC, Marques SFV, Floss MF, Festugato L (2017) Broad-spectrum empirical correlation determining tensile and compressive strength of cement bonded clean granular soils. J Mater Civ Eng 29(6):06017004

Consoli NC, Thome A, Donato M, Graham KS (2008) Loading tests on compacted soil-bottom ash-carbide lime layers. Proc Inst Civ Eng Geotech Eng 161(1):29–38 Consoli NC, Viana da Fonseca A, Cruz RC, Heineck KS (2009a) Fundamental parameters for the stiffness and strength control of artificially cemented sand. J Geotech Geoenviron Eng 135(9):1347–1353

Consoli N.C.; Cruz, R. C.; Consoli, B. S.; Maghous, S. Failure envelope of artificially cemented sand. Géotechnique, v. 62, n. 00, p. 1–5, 2012a.

Consoli N.C.; da Fonseca, A. V.; Silva, S. R.; Cruz, R. C.; Fonini, A. Parameters controlling stiffness and strength of artificially cemented soils. Géotechnique, v. 62, n. 2, p. 177-183, 2012b.

Diambra A, Ibraim E, Festugato L., Corte, MB. (2019). Stiffness of artificially cemented sands: insight on characterisation through empirical power relationships. Road Materials and Pavement Design, 1–11. https://doi.org/10.1080/14680629.2019.1705379

Diambra A, Ibraim E, Peccin A, Consoli NC, Festugato L (2017) Theoretical derivation of artificially cemented granular soil strength. J Geotech Geoenviron Eng 143(5):04017003

Diambra A, Festugato L, Peccin da Silva A, Consoli NC, Ibraim E (2018) Modelling tensile/compressive strength ratio of artificially cemented clean sands. Soils Found 58(1):199–211

Diambra, A.; Ibraim, E. Fibre-reinforced sand: interaction at the fibre and grain scale. Géotechnique, v. 64, n. 4, p. 296–308, 2015. https://doi.org/10.1680/geot.14.P.206

Diambra, A.; Ibraim, E.; Festugato, L.; Corte, M. B. Stiffness of artificially cemented sands: insight on characterisation through empirical power relationships, Road Materials and Pavement Design, 2019. https://doi.org/10.1080/14680629.2019.1705379

Diambra, A.; Ibraim, E.; Muir Wood, D.; Russell, A. R. Fibre reinforced sands: experiments and modelling. Geotextiles and Geomembranes, v. 28, n. 3, p. 238–250, 2010. https://doi.org/10.1016/j.geotexmem.2009.09.010

Diambra, A.; Ibraim, E.; Peccin, A.; Consoli, N. C.; Festugato, L. Theoretical derivation of artificially cemented granular soil strength. Journal of Geotechnical and Geoenvironmental Engineering, v. 143, n. 5, 04017003, 2017. https://doi.org/10.1061/(ASCE)GT.1943-5606.0001646

Diambra, A.; Ibraim, E.; Peccin, A.; Consoli, N. C.; Festugato, L. Theoretical derivation of artificially cemented granular soil strength. Journal of Geotechnical and Geoenvironmental Engineering, v. 143, n. 5, p. 1–9, 2017. https://doi.org/10.1061/(ASCE)GT.1943-5606.0001646

Diambra, A.; Ibraim, E.; Russel, A.; Wood, D. M. Fibre reinforced sands: from experiments to modelling and beyond. Int. J. Numer. Analyt. Methods Geomech, v. 37, p. 2427–2455, 2013. https://doi.org/10.1002/nag.2142

Diambra, A.; Ibraim, E.; Russel, A.; Wood, D. M. Modelling the undrained response of fibre reinforced sands. Soils and Foundations, v. 51, n. 4, p. 625-636, 2011. https://doi.org/10.3208/sandf.51.625

Ladd RS (1967). Preparing test specimens using undercompation. Geotechnical Testing Journal 1(1)40–57

Mitchell JK (1981) Soil improvement—state-of-the-art report. In: Proceedings 10th international conference on soil mechanics and foundation engineering. International Society of Soil Mechanics and Foundation Engineering, Stockholm, pp 509–565